

---

## **Shape and sizing optimisation of automotive structures with deterministic and probabilistic design constraints**

---

**Masoud Rais-Rohani\***

Center for Advanced Vehicular Systems,  
Department of Aerospace Engineering,  
Mississippi State University,  
Mississippi State, MS 39762, USA  
E-mail: masoud@ae.msstate.edu  
\*Corresponding author

**Kiran N. Solanki**

Center for Advanced Vehicular Systems,  
Mississippi State University,  
Mississippi State, MS 39762, USA  
E-mail: kns3@cavs.msstate.edu

**Erdem Acar**

Department of Mechanical Engineering,  
TOBB University of Economics and Technology,  
Söğütözü, Ankara 06560, Turkey  
E-mail: eacar@etu.edu.tr

**Christopher D. Eamon**

Department of Civil and Environmental Engineering,  
Wayne State University,  
Detroit, MI 48202, USA  
E-mail: eamon@eng.wayne.edu

**Abstract:** This paper presents the results of a study on the combined shape and sizing optimisation of automotive structures while examining the effects of different design constraints and associated uncertainties on reliability and efficiency of the optimum designs. Nonlinear transient dynamic finite element analysis is used for full- and offset-frontal crash simulations of a full vehicle model. Surrogate models are developed for the intrusion distance and peak acceleration responses at different vehicle locations based on the material and geometric characteristics of the rail component. The obtained solutions provide insight on the effect of uncertainties in optimum design of automotive structures.

**Keywords:** RBDO; reliability-based design optimisation; automotive crashworthiness; metamodelling; structural reliability; mesh morphing; shape and sizing optimisation; crash simulation; automotive structural design; probabilistic design; vehicle design.

**Reference** to this paper should be made as follows: Rais-Rohani, M., Solanki, K.N., Acar, E. and Eamon, C.D. (2010) 'Shape and sizing optimisation of automotive structures with deterministic and probabilistic design constraints', *Int. J. Vehicle Design*, Vol. 54, No. 4, pp.309–338.

**Biographical notes:** Masoud Rais-Rohani is a Professor in the Department of Aerospace Engineering and leads the simulation-based design optimisation research at Center for Advanced Vehicular Systems at Mississippi State University. He received his PhD in Aerospace Engineering from Virginia Tech in 1991. His areas of teaching include analysis and design of aerospace structures, structural mechanics and engineering design optimisation. His areas of research include computer-aided engineering, engineering design optimisation and uncertainty quantification in design.

Kiran N. Solanki is an Assistant Research Professor at the Center for Advanced Vehicular Systems at Mississippi State University. He received his PhD in Mechanical Engineering from Mississippi State University in 2008. His research efforts are centred on multiscale material modelling, automotive crash simulations and uncertainty characterisation of metallic materials.

Erdem Acar is an Assistant Professor of Mechanical Engineering at the TOBB University of Economics and Technology. He received his PhD in Aerospace Engineering from the University of Florida in 2006, and worked as a Post-Doctoral Research Associate at the Center for Advanced Vehicular Systems at Mississippi State University from 2006 to 2008. His primary areas of teaching include analysis and design of aerospace structures and engineering design optimisation. His research efforts are focused on design optimisation of structural and multidisciplinary systems, structural reliability and metamodelling techniques.

Christopher D. Eamon was an Associate Professor of Civil and Environmental Engineering at Mississippi State University before joining the Lawrence Technological University in 2008, where he is currently an Associate Professor of Civil Engineering. He received his PhD in Civil Engineering from the University of Michigan in 2000. His primary areas of teaching include finite element analysis and structural mechanics. His research efforts include reliability-based design optimisation of structural systems, structural design and non-linear finite element analysis.

---

## 1 Introduction

The rising costs of fossil fuel along with the growing concerns over auto emissions have renewed efforts aimed at enhancing the auto fuel economy. One major contributor to the auto fuel efficiency is the vehicle's weight. During the past several years, the US Department of Energy has sponsored many studies in the area of Automotive Lightweighting Materials (2007) under the Vehicle Technologies Program to investigate the application of materials such as aluminium, magnesium, advanced high-strength steel

and polymer composites in combination with improvements in structural design and manufacturing for reducing the weight of vehicle structures. Examples of some of the sponsored research activities include the Lightweight Front End Structures and Future Generation Passenger Compartment projects. Of course, the challenge in automotive lightweighting is to reduce the structural weight without compromising the crashworthiness standards as articulated in the US Federal Motor Vehicle Safety Standards (FMVSS) and Regulations (Federal Motor Vehicle Safety Standards and Regulations, 1998) or complicating the manufacturing process resulting in increased production cost.

Through mathematical modelling and systematic modification of the structural shape and sizing parameters, it would be possible to optimise the vehicle structure for increased efficiency while satisfying the constraints on crashworthiness and passenger injury criteria. However, besides the objective function(s), the choice of design constraints and their treatment as *deterministic* or *probabilistic* could alter the resulting optimum design. Whereas in the deterministic approach, factors of safety are commonly used to safeguard against variability, in the probabilistic approach, the sources of stochastic uncertainty are treated as random variables with distinct probability distributions. Besides facilitating a more accurate assessment of structural reliability, the probabilistic approach also accommodates the formulation of the design problem as a Reliability-Based Design Optimisation (RBDO) problem that results in more consistent assessment of failure probability among different structural components or failure modes in comparison with the deterministic approach.

In this paper, we examine the influence of design constraint formulation on optimum design of automotive structures. While using the FE simulation results of full-vehicle crash to guide the computational design efforts, we will concentrate on the design of only the front rail components, which play an important role in the absorption of impact energy in full- and offset-frontal impact conditions. Besides the engineering properties of the material, the geometric attributes of the rail can have a significant impact on its collapse and energy absorption characteristics. Hence, by controlling the form and rate of plastic deformation during crash, it would be possible to increase energy absorption and reduce the peak acceleration in the passenger compartment. The selected responses of interest in this problem are the intrusion distance and peak acceleration at three different vehicle locations. While changes in component geometry can influence its manufacturability, no constraints on manufacturability or production cost have been considered in this study.

A very challenging aspect of combining numerical optimisation with FE crash simulations and structural reliability analysis is the overall computational requirement as well as the numerical noise that is often present in a calculated transient dynamic response such as acceleration. To alleviate this problem, the metamodelling approach is used to build separate surrogate models for the crash responses of interest. The resulting smooth analytical functions are then coupled with design optimisation and structural reliability analysis to find the optimum rail geometry for different combinations of objective function and design constraints in the presence of design uncertainties.

As with many other realistic engineering problems, the example problem chosen here is complex, and as such, the competing design criteria may produce results that are not intuitive. Thus, it is necessary to consider multiple test cases to fully quantify the impact of problem formulation on the optimum design.

The remaining portion of the paper is organised as follows. Sections 2 and 3 describe the deterministic and probabilistic optimisation approaches and the potential strategies to increase the efficiency of reliability analysis and the solution of RBDO problems. Sections 4 and 5 describe the underlying methodology for crash simulation and metamodelling whereas Section 6 gives a thorough description of the side-rail example problem including a comparison of deterministic and probabilistic optimisation results. Concluding remarks appear in Section 7.

## 2 Deterministic Design Optimisation

In a generic formulation of the Deterministic Design Optimisation (DDO) problem, we seek the optimal values of design variables in vector  $\mathbf{Y}$  that would

$$\begin{aligned} & \min f(\mathbf{Y}) \\ & \text{s.t. } g_i(\mathbf{Y}) \leq 0; \quad i = 1, N_g \\ & Y_k^l \leq Y_k \leq Y_k^u; \quad k = 1, \text{NDV} \end{aligned} \quad (1)$$

where  $f(\mathbf{Y})$  is the objective function,  $g_i$  is the  $i$ th inequality constraint, and  $Y_k$  is the  $k$ th design variable with lower and upper bounds (side constraints),  $Y_k^l$  and  $Y_k^u$ , respectively. When design variables represent continuous (e.g., shape and sizing) variables, the solution to equation (1) can be found using a mathematical programming method such as the Modified Method of Feasible Directions (MMFD) (Vanderplaats, 1999) or the Sequential Quadratic Programming (SQP) (Rao, 1996). In these methods, the original functions and their gradients are used in the formulation of an approximate subproblem for finding the components of the search direction vector at the current design point. Following the determination of optimum step size along the selected search direction, an updated (improved) design point is identified. The procedure is repeated until solution converges to an optimal design point. When a problem is non-convex, the optimisation problem is often solved by considering multiple initial design points with the best design identified from the set of locally optimum solutions.

When the optimisation problem involves multiple objectives,  $f(\mathbf{Y})$  in equation (1) is modified to  $f(\mathbf{Y}) = [f_1(\mathbf{Y}), f_2(\mathbf{Y}), \dots, f_{N_f}(\mathbf{Y})]$ . Since in many problems the objective functions are in conflict, it is impossible to find a vector  $\mathbf{Y}$  that optimises all the objective functions simultaneously. Hence, a compromise or Pareto optimum solution is sought. Many methods have been developed for the solution of multi-objective design optimisation problems including the utility function method, bounded objective function method, global criterion method and compromise programming approach (Rao, 1996). In compromise programming,  $f(\mathbf{Y})$  is expressed as

$$f(\mathbf{Y}) = \left\{ \sum_{m=1}^{N_f} \left[ \frac{w_m (f_m(\mathbf{Y}) - f_m^t(\mathbf{Y}))}{f_m^w(\mathbf{Y}) - f_m^t(\mathbf{Y})} \right]^2 \right\}^{0.5} \quad (2)$$

where the superscripts  $t$  and  $w$  denote the target and worst values, respectively, for each objective function with  $w_m$  representing a scalar weight factor associated with the  $m$ th objective function.

In equation (1), all design variables and constraints have deterministic values, and design uncertainties are addressed only in a very limited fashion with the use of factors of safety on material properties and constraint limits. As such, the resulting optimum design can have inconsistent levels of failure probability among the failure modes, with some being unexpectedly high, especially in the presence of active design constraints. For consistent levels of failure probability and quantitative modelling of design uncertainties, the deterministic formulation in equation (1) is replaced by a probabilistic or RBDO formulation as discussed in the following section.

### 3 Reliability-Based Design Optimisation

The underlying stochastic uncertainties in product design can be represented in terms of an  $n$ -dimensional vector of random variables,  $\mathbf{X} = \{X_1, X_2, \dots, X_n\}^T$  with each variable having a continuously differentiable cumulative distribution function,  $F_x(\mathbf{X})$ .

If  $G(\mathbf{X}, \mathbf{Y})$  represents a stochastic response function for measuring product performance, then the failure condition is defined as  $G(\mathbf{X}, \mathbf{Y}) \leq 0$  whereas  $G(\mathbf{X}, \mathbf{Y}) > 0$  implies safety with  $G(\mathbf{X}, \mathbf{Y}) = 0$  representing the limit-state surface that separates the safe and failure regions of the random-variable space. For this response function, the probability of failure is defined as the probability of  $G(\mathbf{X}, \mathbf{Y}) \leq 0$ , which can be computed using the multi-integral equation

$$P_f = P[G(\mathbf{X}, \mathbf{Y}) \leq 0] = \int_{G(\mathbf{X}, \mathbf{Y}) \leq 0} f_x(\mathbf{X}) d\mathbf{X} \quad (3)$$

where  $P_f$  is the failure probability and  $f_x(\mathbf{X})$  is the joint probability density function of random variables integrated over the failure domain of random variables.

There are alternative ways of formulating a stochastic non-linear programming (Rao, 1996) or RBDO problem (Enevoldsen and Sorensen, 1994; Frangopol, 1995; Tu et al., 1999). In a generic RBDO problem, we seek the optimal vector of design variables  $\mathbf{Y} = \{Y_1, Y_2, \dots, Y_{\text{NDV}}\}^T$  that would

$$\begin{aligned} & \min f(\mathbf{X}, \mathbf{Y}) \\ & \text{s.t. } P_{f_i} = P[G_i(\mathbf{X}, \mathbf{Y}) \leq 0] \leq P_{a_i}; \quad i = 1, N_p \\ & Y_k^l \leq Y_k \leq Y_k^u; \quad k = 1, \text{NDV} \end{aligned} \quad (4)$$

where  $P_{a_i}$  represents the allowable value or upper bound on the  $i$ th failure probability,  $P_{f_i}$ , for a single event that may be represented by a unique failure mode in a structural component or a system. The probabilistic constraint set in equation (4) may include both component- and system-level reliabilities with each constraint limit related to the corresponding target reliability index defined as  $\beta_{t_i} = -\Phi^{-1}(P_{a_i})$ , where  $\Phi(\cdot)$  is the standard normal cumulative distribution function. Although  $\mathbf{X}$  and  $\mathbf{Y}$  in equation (4) describe two separate vectors, the mean values of random variables  $\mu_x$  are often chosen as the design variables.

For a trade-off between design efficiency and robustness, the objective function in equation (4) can be written in its equivalent deterministic form as  $f(\mathbf{X}, \mathbf{Y}) = a_1 \mu_f(\mathbf{X}, \mathbf{Y}) + a_2 \tilde{\sigma}_f(\mathbf{X}, \mathbf{Y})$ , where  $\mu_f$  and  $\tilde{\sigma}_f$  represent the mean and standard

deviation values, respectively, of  $f(\mathbf{X}, \mathbf{Y})$  while the coefficients  $a_1$  and  $a_2$  denote scalar weighting factors that signify the desired emphasis on efficiency and robustness, respectively (Rao, 1992). As in the case of equation (1), it is also possible to have multiple objective functions in equation (4).

In RBDO of structural components, design uncertainties associated with material properties and loading condition as well as the component shape and sizing are captured in the mathematical formulation and solution of the optimisation problem.

As is often the case, some responses may be marginally impacted or totally unaffected by the variability in the random variables (i.e., design uncertainties), and consequently they can be treated as deterministic. If, for instance, the objective function and a subset of design constraints are deterministic, then equation (4) can be rewritten as

$$\begin{aligned} & \min f(\mathbf{Y}) \\ & \text{s.t. } g_i^p(\mathbf{X}, \mathbf{Y}) = \frac{P[G_i(\mathbf{X}, \mathbf{Y}) \leq 0]}{\Phi(-\beta_i)} - 1 \leq 0; \quad i = 1, N_p \\ & g_j^d(\mathbf{Y}) = \frac{R_{c_j}(\mathbf{Y})}{R_{a_j}} - 1 \leq 0; \quad j = 1, N_d \\ & Y_k^l \leq Y_k \leq Y_k^u; \quad k = 1, \text{NDV} \end{aligned} \quad (5)$$

where  $g_i^p$  and  $g_j^d$  represent normalised reliability-based and deterministic constraints, respectively, with the latter preventing the critical value of a deterministic response,  $R_{c_j}$ , from exceeding its allowable value,  $R_{a_j}$ .

The presence of probabilistic design constraints makes the solution of equation (5) more challenging and expensive than that of equation (1). Different approaches for the evaluation of  $g_i^p(\mathbf{X}, \mathbf{Y})$  have been developed. In the reliability index approach (Enevoldsen and Sorensen 1994),  $g_i^p(\mathbf{X}, \mathbf{Y})$  is described in terms of a lower bound on the reliability index (i.e.,  $g_i^p(\mathbf{X}, \mathbf{Y}) = 1 - \beta_i(\mathbf{X}, \mathbf{Y}) / \beta_i \leq 0$ , where  $\beta_i(\mathbf{X}, \mathbf{Y}) = -\Phi^{-1}(P[G_i(\mathbf{X}, \mathbf{Y}) \leq 0])$ ) whereas in the performance measure approach (Tu et al., 1999), it is modelled using inverse transformation (i.e.,  $g_i^p(\mathbf{X}, \mathbf{Y}) = -F_{G_i}^{-1}(\Phi(-\beta_i)) \leq 0$ , where  $F_{G_i}(0) = P[G_i(\mathbf{X}, \mathbf{Y}) \leq 0]$ ). More recently, Du and Chen (2004) proposed the replacement of  $g_i^p(\mathbf{X}, \mathbf{Y})$  with an equivalent deterministic constraint and the decoupling of reliability analysis and design optimisation in each design cycle whereas Qu and Haftka (2004) suggested the use of probability safety factor in modelling each probabilistic constraint.

In general, the solution to the RBDO problem in equation (4) or equation (5) involves two major parts: the search for the optimum design point in the design-variable space, and the evaluation of component failure probability (or reliability index) in the random-variable space at every updated design point. Whether these two parts are kept separate or combined in some fashion, the efficient solution of RBDO of complex systems requires the use of approximation techniques in one or more areas including the modelling of limit state functions, the evaluation of structural reliability and the determination of optimum design.

### 3.1 Approximate methods for reliability analysis

For most engineering problems, the analytical integration of equation (3) or the full distributional approach is not possible; hence, many simulation and approximate analytical methods have been developed for component reliability estimation.

Simulation-based methods include the direct Monte Carlo Simulation (MCS) (Rubinstein, 1981) and its more advanced variants such as Importance Sampling (Melchers, 1989), Adaptive Importance Sampling (Wu, 1994) and Directional Simulation (Nie and Ellingwood, 2000). Depending on the extent of sampling of the failure domain, the results obtained from simulation-based methods may represent approximate reliabilities.

Analytical methods, which include the popular First- and Second-Order Reliability Methods (FORM and SORM), involve the transformation of random variables and approximation of non-linear limit-state function for the determination of the Most Probable Point (MPP) of failure and the reliability index,  $\beta$ . In structural reliability, MPP represents the maximum value on the joint probability density function that lies on the limit-state surface in standard normal space, whereas the distance from the origin of the coordinate system to MPP represents  $\beta$  (Hasofer and Lind, 1974).

Since the search for MPP can be treated as an optimisation problem, many solution techniques have been developed for its calculation (Hasofer and Lind, 1974; Rackwitz and Fiessler, 1978; Der Kiureghian et al., 1987) with a comparison of different algorithms given by Liu and Der Kiureghian (1991). Other approximate reliability analysis methods include the Fast Probability Integration (Wu and Wirsching, 1987), Advanced Mean Value method (Wu and Burnside, 1988) and its more accurate variant (AMV+) (Wu et al., 1990). To increase the efficiency of FORM, Wang and Grandhi (1994) introduced intervening variables for approximation of non-linear limit-state functions. More recently, Acar et al. (2010) combined the Univariate Dimension Reduction approach of Rahman and Xu (2004) with the Extended Generalised Lambda Distribution (EGLD) fitting of Karian et al. (1996) to develop an analytical approach that does not require the calculation of MPP for reliability estimation.

Although – depending on the form of the limit-state function and the number of random variables involved – the analytical methods tend to be less accurate than the simulation-based methods, they are more computationally efficient, especially when combined with numerical optimisation for RBDO of complex systems. For a survey of reliability analysis methods, the reader is referred to Rackwitz (2001).

In this study, we chose the AMV+ method for reliability analysis, where the first-order Taylor series expansion of the limit-state function is performed at the MPP instead of the mean value point. Since the location of MPP is not readily available, AMV+ uses an iterative procedure for its calculation and that of the probability of failure. Even though AMV+ method typically requires additional samples than the more traditional methods such as FORM, it yields better accuracy for non-linear limit-state functions, such as those encountered in vehicle crash simulations. We developed a MATLAB function for the implementation of the AMV+ method for reliability assessment.

### 3.2 *Approximate methods for RBDO*

Most approaches for solving the RBDO problem in equation (4) or equation (5) employ at least one form of approximation. The most common solution techniques employ a nested or double-loop procedure, wherein the reliability analysis constitutes the inner loop and the design optimisation the outer loop. Other methods involve either sequential or single-loop (unilevel) procedures. A brief overview of some of the suggested solution techniques as published over the last decade is presented in this section.

To increase the solution efficiency, Grandhi and Wang (1998) replaced the exact limit-state function with a two-point adaptive non-linear approximation while using FORM for the reliability analysis. Kirjner-Neto et al. (1998) proposed an outer approximation of the optimum solutions for the reliability analysis part. Yu et al. (1997) developed a mixed design approach in which a FORM-based RBDO is performed only if the deterministic optimum solution does not provide a satisfactory level of reliability. Koch and Kodiyalam (1999) proposed a variable-complexity technique in which the accuracy of FORM solutions is balanced with more efficient solutions derived from the Mean-Value First-Order Reliability Method (MVFORM) through the so-called adjustment factors.

Lee and Kwak (1995) suggested replacing MPP-search optimisation with Neumann expansion technique. Papadrakakis and Lagaros (2002) used the combination of neural networks and evolution strategies to develop inexpensive estimates of deterministic and probabilistic constraints and used MCS based on Importance Sampling for the reliability analysis. Kharmanda et al. (2002) developed a technique to combine the design and random variables into a single albeit more complex Hybrid Design Space (HDS) for a simultaneous (single-loop) solution of the reliability and optimisation problems. The proposed HDS-based method is shown to be much more computationally efficient when compared with the traditional double-loop procedure. Mohsine et al. (2004) extended the HDS-based method to what they call the Improved Hybrid Method (IHM) by including standard deviations as optimisation variables, and showed an improvement in the optimum design from the same starting point. Kharmanda et al. (2004) introduced the Optimum Safety Factor (OSF) approach that relies on the first-order Karush-Kuhn-Tucker (KKT) optimality criteria for the solution of RBDO problems at a reduced computational cost. The OSF approach was later applied to problems involving highly non-linear and non-normal random variables (Kharmanda and Olhoff, 2007).

Choi et al. (2001) introduced a general Design Potential Concept (DPC) for RBDO with smooth and non-smooth probabilistic constraints. They described DPC as searching for the minimum cost design in the unified design space, which is obtained by mapping the design space into system parameter space and transforming it into the standardised normal reference space. They also provided the extension of DPC for extreme cases, for instance the structures with very small probability of failure. Youn and Choi (2004a) compared the reliability index, approximate moment and PMAs for modelling of reliability constraints in RBDO and suggest that the PMA is less prone to numerical instability than the other two approaches while providing more accurate solutions for non-linear limit-state functions. Yang and Gu (2004) investigated four different approximate RBDO strategies and found that the Single-Loop-Single-Vector (SLSV) approach of Chen et al. (1997) provides the best solution in terms of accuracy and efficiency.

Zou and Mahadevan (2006) proposed a decoupled approach to solve an RBDO problem by using a first-order Taylor series approximation of failure probabilities to formulate a deterministic set of reliability constraints and solving an approximate deterministic optimisation problem. After each deterministic optimisation, a more accurate reliability analysis (e.g., MCS) is performed only for the active reliability constraints. Through the application of potential constraint strategy and sequential approximate optimisation, the RBDO problem is solved with comparable efficiency to PMA. Agarwal et al. (2007) have replaced the inverse FORM in PMA with its KKT conditions at the upper-level optimisation problem and show that the new approach is more robust with better convergence characteristics in comparison with the procedure developed by Kuschel and Rackwitz (2000).

In this study, we chose the double-loop procedure based on the reliability index approach. The reason for this choice is the simplicity and the reasonable accuracy of this procedure when the response functions of interest are approximated using closed-form analytical functions (i.e., metamodels).

### *3.3 RBDO of automotive components*

The desire to improve design safety and efficiency in the presence of various sources of uncertainty has led to the growth of probabilistic design modelling and RBDO in automotive applications. Liaw and DeVries (2001) discuss the effects of uncertainty in design variables on the variability of different vehicle responses and the use of this information to find robust optimum designs. They modelled variability using two metamodeling techniques: Forward Stepwise Regression (FSR) and Enhanced Multivariate Adaptive Regression Splines. They examined the trade-off between weight and target reliability in one vehicle design problem where durability, noise and vibration are taken as responses of interest with panel thicknesses and elastomer stiffness treated as the design and random variables. Zhang and Liu (2002) used the probabilistic perturbation method together with the Mean-Value First- and Second-Order Method (MVFORM, MVSORM) for reliability analysis and design (no optimisation) of nine different automotive components including a tension bar, connecting rod, semi-axle, fore-axle and torsion bar. In all problems, the limit state functions are in analytical form expressed in terms of two to seven random variables. Yang et al. (2004) presented the recent developments and applications of structural safety optimisation and robustness methods for vehicle crashworthiness-based gauge, size, shape and topology optimisation. They encouraged the use of response surface approximations in reliability analysis of vehicle crashworthiness.

Youn and Choi (2004b) combined their proposed Hybrid Mean Value (HMV) method for structural reliability analysis with response surface methodology based on quadratic backward-stepwise regression, and applied the combined approach to RBDO of a vehicle model in side crash. The responses modelled included force, deflection and viscous criterion as experienced by the dummy as well as the intrusion velocities at the door and the B-pillar. An extension of this effort in Youn et al. (2004) gave a comparison of PMA and HMV methods in RBDO solutions with the same side crash model as an example. The nine continuous design variables consisted of wall thickness and material properties. Gu and Yang (2006) discuss different aspects of RBDO in their paper and using the same side crash problem as mentioned earlier examine the characteristics of solutions based on SLSV, MVFORM and their combination with those obtained using SQP

and MCS combination. They found MVFORM to be the most efficient approach with comparable results to SLSV.

Kaymaz and McMahon (2004) proposed a probabilistic design system called ADAPRES\_NET for RBDO problems. The two principal features of the system are: adaptive response surface approximations for reliability analysis using FORM and network programming to distribute the computational tasks. The RBDO of a connecting rod is used as an example problem to show the computational efficiency of the proposed design system.

Yang et al. (2005) extended the work of Yang and Gu (2004) by evaluating the efficiency and accuracy of multiple RBDO methods. An automobile exhaust hanger system defined by four sizing variables was optimised for minimum weight subject to 144 reliability design constraints on resultant force in three different frequency domains. They found that direct application of these methods render them computationally very expensive. They concluded that an active constraint strategy combined with a hybrid approach for approximate optimisation can improve the computational efficiency in reliability design. Sinha (2007) presented a methodology for reliability-based multidisciplinary optimisation of engineering structures. He applied this methodology to design optimisation of vehicle structures for crashworthiness and occupant safety in side impact. The probabilistic constraints were calculated using FORM. Pareto frontier was generated for showing the trade-offs between vehicle weight and door intrusion velocity.

It is worth noting that in all the vehicle design optimisation problems cited earlier, the design modifications do not include changes to the product shape, which requires the altering of the FE mesh to determine the effect of shape change on response functions of interest in the design optimisation problem.

#### **4 Crash simulation**

Crash characteristics are measured by various performance parameters including intrusion distance, strain energy, strain-energy absorption rate, peak acceleration and its profile, and contact force. One critical factor is the amount of energy transferred to the occupants, which is directly proportional to the amount of energy absorbed by the vehicle structure during a crash scenario. Ideally, vehicle simulation models would include human (or dummy) models to predict various bodily injuries to the occupants. However, in the absence of such models, average responses at key passenger compartment locations are used as surrogates or secondary risk measures.

Non-linear transient dynamic FEA based on explicit time integration schemes has proven to be a powerful computational tool in analysing the large-deformation dynamic responses of vehicle models in various crash events. Commercial codes, such as LS-DYNA, PAM-CRASH, ABAQUS and RADIOSS, are widely used in performing realistic and predictive virtual crash simulations. Here, crash simulations are performed using LS-DYNA MPP v970.

#### **5 Metamodelling**

A single high-fidelity vehicle crash simulation for a brief time period of approximately 100 ms could take in excess of 10 CPU hours even on a multiprocessor-based parallel

computing platform (Fang et al., 2005; Rais-Rohani et al., 2006). Moreover, crash response characteristics such as peak acceleration can be non-smooth (noisy), which prevents their use in gradient-based design optimisation solutions. Therefore, the application of DDO and RBDO to vehicle design problems requires the use of smooth approximate functions for increased computational accuracy and efficiency.

One method of approximation is to develop surrogate models (metamodels) for estimation of the responses of interest. There are several advantages to using metamodels including the elimination of noise in some responses such as acceleration, the fast and low-cost computation of responses during the optimisation process, and the evaluation of exact derivatives using closed-form analytical functions. Metamodels generally tend to enhance the efficiency of both the reliability analysis as well as the design optimisation.

Metamodelling or response surface techniques have been used in numerous engineering applications (e.g., Daberkow and Mavris, 2002; Rais-Rohani and Singh, 2004) in recent years. Detail information about various metamodelling techniques and the performance of the resulting models in approximating non-linear and complex multivariate functional relationships can be found in recent survey papers (Simpson et al., 1998, 2001; Jin et al., 2001). More recent efforts include the use of weighted-sum formulation of two or more metamodels to create an ensemble of approximate functions. By taking advantage of the prediction ability of each stand-alone metamodel, it is possible to enhance the accuracy of the response predictions with an ensemble formulation (Goel et al., 2007; Acar and Rais-Rohani, 2009).

In comparing various parametric and non-parametric metamodels for some 20 different benchmark problems, Wang et al. (2006) have shown that, based on six separate performance criteria, the multiquadric Radial Basis Functions (RBFs) outperformed other metamodels, such as quadratic Response Surface and Multivariate Adaptive Regression Splines (MARS), for highly non-linear and non-noisy functions. Fang et al. (2005) also showed that for responses of interest in automobile crash simulations, multiquadric RBF surpasses the more traditional Polynomial Response Surface (PRS) models in terms of prediction accuracy.

On the basis of the previous experience (Fang et al., 2005) and considering the forms of response functions of interest in automobile crash, we focused on two candidate metamodelling techniques, one that provides a parametric regression model (i.e., PRS) and another that results in a non-parametric interpolation model (i.e., RBF).

A general, second-order PRS using a quadratic polynomial can be expressed as

$$\tilde{f}(\mathbf{x}) = a_0 + \sum_{i=1}^m a_i x_i + \sum_{i=1}^m a_{ii} x_i^2 + \sum_{i=1}^{m-1} \sum_{j=i+1}^m a_{ij} x_i x_j \quad (6)$$

where  $m$  is the total number of input variables,  $x_i$  is the  $i$ th input variable and the  $a_i$  are the unknown constant coefficients. Depending on the response and the number of input variables, equation (6) is often used either in its complete (fully quadratic) form or with the interaction terms excluded. However, this approach either leads to the inclusion of terms that have minimal influence on the response or the possibility of leaving out an important interaction term. A more efficient alternative is to use an FSR procedure that uses a combination of forward entry and backward removal through which only the influential effects together with the regression intercept are included in the model. For more details about the stepwise model-building techniques, the reader is referred to Darlington (1990).

RBF methods (Buhmann, 2003) were originally developed to approximate multivariate functions based on scattered data. For a data set consisting of the values of input variables and response values at  $n$  sampling points, the true function  $f(\mathbf{x})$  can be approximated as

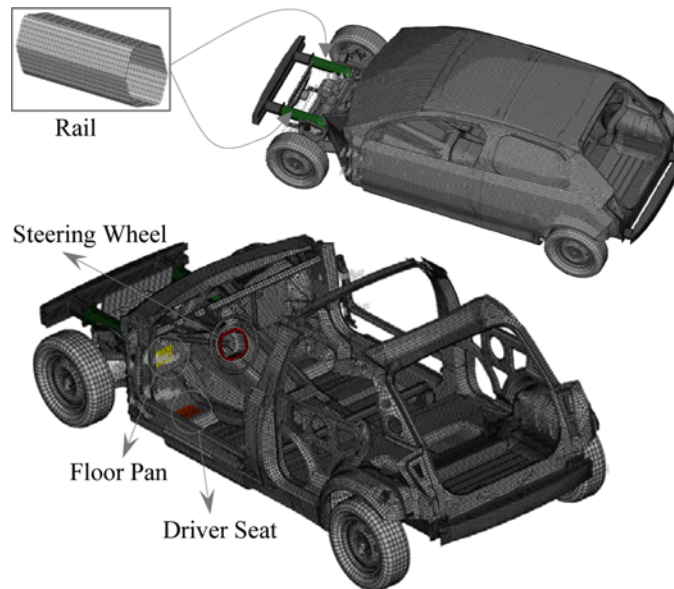
$$\tilde{f}(\mathbf{x}) = \sum_{i=1}^n \lambda_i \phi(\|\mathbf{x} - \mathbf{x}_i\|) \quad (7)$$

where  $\mathbf{x}$  is the vector of input variables,  $\mathbf{x}_i$  is the vector of input variables at the  $i$ th sampling point,  $\|\mathbf{x} - \mathbf{x}_i\| = \sqrt{(\mathbf{x} - \mathbf{x}_i)^T (\mathbf{x} - \mathbf{x}_i)}$  is the Euclidean norm representing the radial distance,  $r$ , from design point  $\mathbf{x}$  to the sampling point or centre  $\mathbf{x}_i$ ,  $\phi$  is a radially symmetric basis function, and  $\lambda_i$ ,  $i = 1, \dots, n$  are the unknown interpolation coefficients. Among the various options for RBF (e.g., thin plate spline, Gaussian, multiquadric and inverse multiquadric), we found the multiquadric formulation,  $\phi(r) = \sqrt{r^2 + c^2}$ , to provide the most accurate predictions for crash responses of interest. The parameter  $c$  in  $\phi(r)$  is a constant such that  $0 < c \leq 1$  when the radial distances are normalised.

## 6 Design application problem

Figure 1 shows a modified version of the full-scale FE model of a c-class passenger car developed by the Partnership for a New Generation of Vehicles team under the UltraLight Steel AutoBody-Advanced Vehicle Concepts (ULSAB-AVC) program group. This vehicle model consists of 313 components, most of which are made of isotropic materials with the non-linear behaviour of material defined by the true stress-strain curves at different strain rates. The baseline design has a mass of approximately 1210 kg.

**Figure 1** Vehicle FE model showing the rail and the locations of measured responses (see online version for colours)



The design effort here is focused on the geometric (i.e., shape and size) optimisation of only the front two rails (see Figure 1) for improved crashworthiness and lightweighting. The rails play a crucial role in attenuating the impact energy in frontal impact. Whereas in the baseline model the rails are straight prismatic members with a hexagonal cross-section, they are allowed to change shape (become non-prismatic) in the optimisation process with varying curvatures in both vertical and horizontal planes. The wall thickness is also allowed to vary in the optimisation process but kept uniform throughout the component. When the component shape is allowed to change, it is necessary to morph the FE mesh repeatedly during the optimisation process. The procedure for mesh morphing is discussed in the next section. Generally speaking, it is much more difficult to change the shape than thickness of structural members in finite-element-based design optimisation problems such as the one considered here.

The selected crash responses are the total intrusion distances and peak accelerations (decelerations times  $-1$ ) at the Floor Pan (FP) (Dis\_FP, Acc\_FP), the Driver Seat (DS) (Dis\_DS, Acc\_DS), and the steering wheel (Dis\_SW, Acc\_SW), with locations identified in Figure 1. The area designated as DS is actually located in the toe pan area of the driver side. To reduce noise in the sampled responses, intrusion distance and acceleration values are averaged over a small area consisting of multiple FEs at the three sites of interest as highlighted in Figure 1. Although reduced intrusion distances are generally favourable, that reduction may be accompanied by dangerously high accelerations ( $g$ -load) experienced by the occupants. Hence, a proper balance must be maintained.

The twofold frontal impact scenarios considered here, i.e., Full Frontal Impact (FFI) and Offset Frontal Impact (OFI), are depicted in Figure 2. In FFI simulation, the vehicle crashes into a rigid wall, whereas in OFI it collides into a deformable barrier supported by a rigid wall. The deformable barrier is made of multiple layers of materials including aluminium honeycomb with overall stiffness properties defined according to FMVSS 208 standards. Since the deformable barrier has greater structural stiffness than the vehicle, its deformation is not as noticeable as that of the vehicle in Figure 2(b). Details of the FE models in FFI and OFI are given in Table 1. The FE model in FFI has mostly Belyschko-Tsay shell elements, for a total of over 1.1M degrees of freedom. In OFI, the deformable barrier model includes additional nodes and elements (76% of which are solid). The average element size in the deformable barrier is 12.5 mm.

Since car crash is a transient event, the desired responses have to be evaluated over a specific time interval beyond initial impact. Figure 3 shows the plots of time variations of peak accelerations and intrusion distances calculated using LS-DYNA and averaged over multiple elements at the three designated sites in the baseline model. The symbol AAA\_BB\_C refers to the response, site and crash scenario, respectively. The plots show that the maximum acceleration occurs at some instant during the first 30 ms time interval following collision with Acc\_DS having the highest value in both impact scenarios. The average intrusion distances, computed by subtracting nodal rigid-body translation from the actual nodal displacement, are also shown in Figure 3. The intrusion distance calculations are based on the same procedure as that described in Fang et al. (2004). The plot shows that the intrusion distance, Dis\_FP, has the largest average value at approximately 100 ms. It is worth noting that although some of the curves for intrusion distance have an upward trend, they level off or drop shortly after the 100 ms time is reached.

**Table 1** Summary of FE models for frontal crash simulations

Model	Node	Elements				Impact time (ms)
		Solid	Shell	Beam	Total	
FFI	184,436	1,072	178,414	358	179,844	100
OFI	351,618	158,592	227,054	358	386,004	100

**Figure 2** Baseline vehicle model before and after (a) full-frontal impact with a rigid wall and (b) offset-frontal impact with a deformable barrier

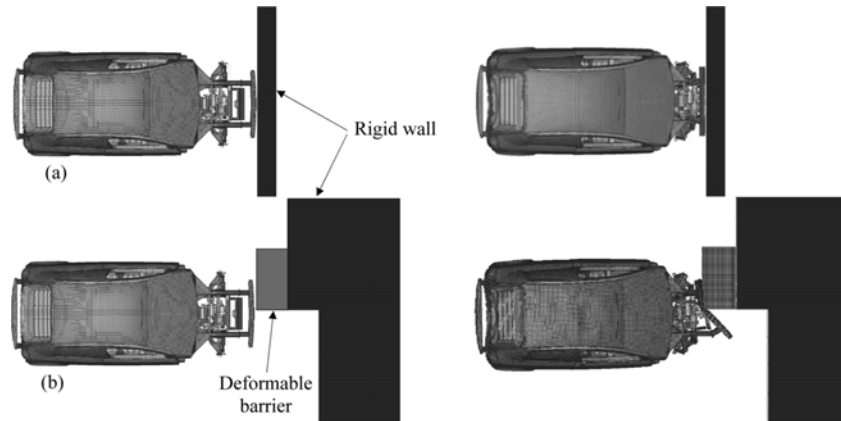
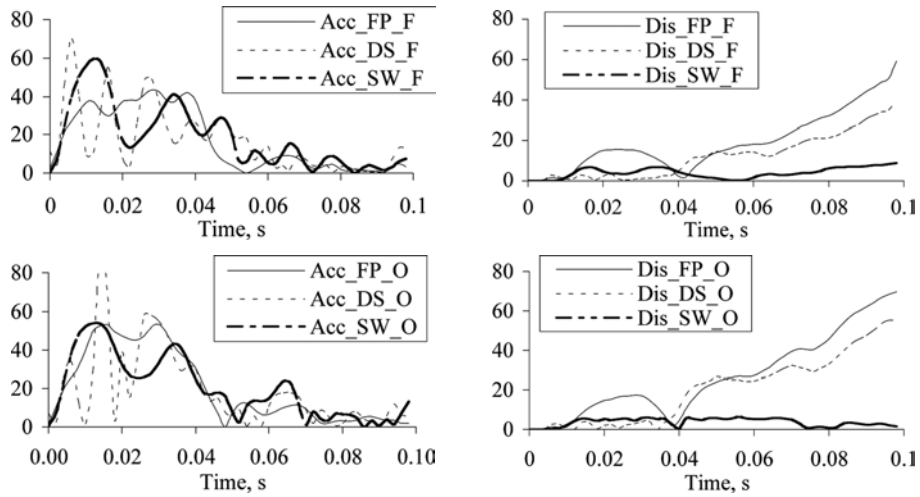


**Figure 3** Average acceleration and intrusion distance variations in regions of interest in the baseline model



Crash simulations of full-vehicle models require substantial computational resources due to iterative non-linear transient dynamic FEA procedure at computational time steps in the order of 1.0E-06. For instance, a 100-ms OFI simulation of the baseline model takes approximately 17 CPU hours with LS-DYNA MPP v970 using 32 processors on an IBM Linux Cluster with Intel Pentium III 1.266 GHz processors and 607.5 GB RAM. By comparison, a comparable FFI simulation takes approximately 13 CPU hours.

### 6.1 Mesh morphing

If the model is allowed to change shape during design optimisation, then it is necessary to modify the FE mesh to correctly capture the influence of such change on structural response. This modification may involve developing a whole new mesh for each design perturbation or morphing (reshaping) the original mesh. We chose the latter approach, and kept the numbers of nodes and elements as well as element connectivity fixed while allowing the coordinates of a particular subset of nodes (i.e., deformable nodes) to change. There are various ways of adjusting the nodal coordinates. One approach is to start with a series of configurations (i.e., basis vectors) that are different only in regions where the shape can change, and then find the necessary contribution from each basis vector that would optimise the component design. Another approach is to group specific nodes in a region of interest into a domain and to apply perturbation vectors at specific nodes of the domain.

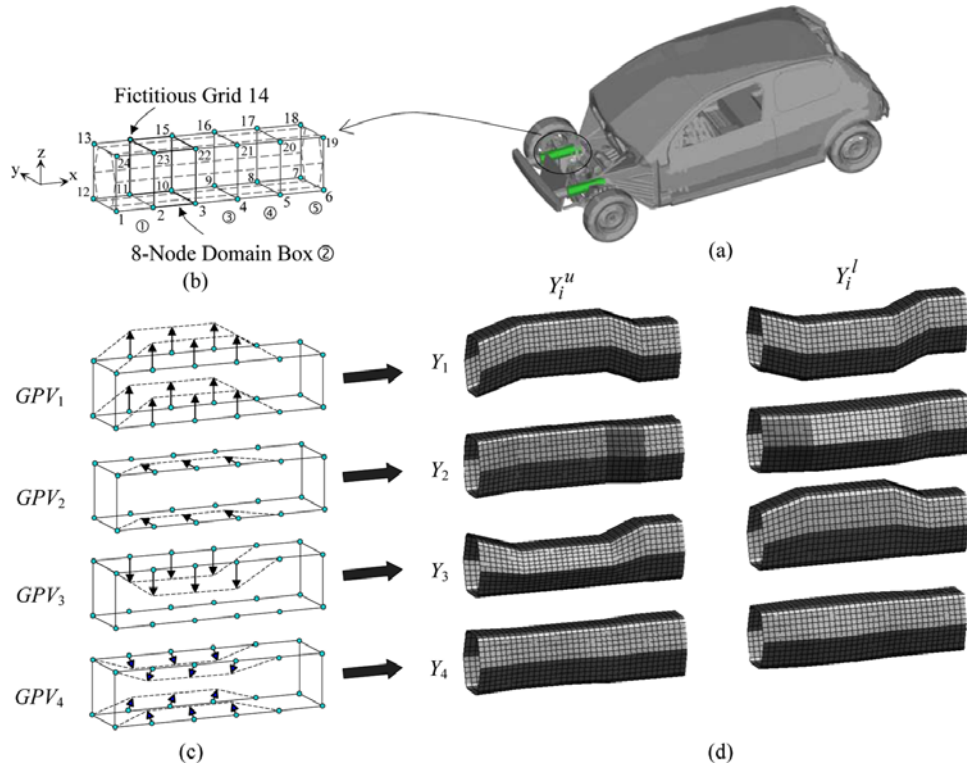
To simplify the perturbation of the baseline geometry, each rail is enclosed inside a fictitious rectangular box. Figure 4(b) shows this arrangement for a single rail. The rectangular box is divided lengthwise into five smaller boxes (domains 1–5) with the coordinates of each of its eight corners defined by that of the corresponding fictitious node as shown in Figure 4(b). The fictitious nodes do not enter the FEA, and are only used to control the coordinates of grid nodes in the underlying structure as the shape of each domain is perturbed. By defining the location, direction and magnitude of each Geometric Perturbation Vector (GPV) in a given set, we will specify how the geometry of each domain as well as that of the enclosed rail will be morphed. The fictitious nodes associated with both rails are perturbed in a consistent manner to maintain symmetry between the two rails. Four GPV sets are considered in this problem with their points of application and positive direction as shown in Figure 4(c).

The nodal coordinates of the perturbed FE mesh are determined as

$$\begin{Bmatrix} x_i^{(p)} \\ y_i^{(p)} \\ z_i^{(p)} \end{Bmatrix} = \begin{Bmatrix} x_i^{(o)} \\ y_i^{(o)} \\ z_i^{(o)} \end{Bmatrix} + \sum_{j=1}^4 Y_j \begin{Bmatrix} x_i^{(j)} - x_i^{(o)} \\ y_i^{(j)} - y_i^{(o)} \\ z_i^{(j)} - z_i^{(o)} \end{Bmatrix} \quad (8)$$

where subscript  $i$  identifies the FE node number, superscripts  $o$  and  $p$  refer to the original and perturbed mesh, respectively, and  $Y_j$  represents the value of the  $j$ th shape design variable. It is important to note that  $Y_j$  could have negative values within the side constraints specified in the optimisation problem. While the magnitude of the shape design variable has a scaling effect on the corresponding GPV, its sign defines the direction of perturbation vectors. At the extreme values of  $Y_j, j = 1, \dots, 4$ , the geometry of the rail will take the shapes shown in Figure 4(d). Because of connection with the bumper at the one end and the body structure at the other end, the nodal locations at the right and left ends of the rails are kept fixed. Depending on the desired shape change, adjustments can be made to the number of GPV sets, the location and axis of each perturbation vector, as well as the number and set-up of morphing domains. It should be noted that for the rail shape modification only the  $y$  and  $z$  components of the nodal coordinates are changed. Hence, in equation (8), the  $x$ -coordinates do not change, i.e.,  $x_i^{(p)} = x_i^{(o)}$ .

**Figure 4** (a) Right rail; (b) fictitious box enclosing the rail mesh; (c) geometric perturbation vectors pointing in the positive direction, and (d) perturbed mesh corresponding to the upper (+) and lower (–) bounds of shape design variables  $Y_1$  through  $Y_4$  (see online version for colours)



The mesh perturbation (morphing) is performed by combining an in-house programme and the GENESIS (2005) software. The mesh smoothing option in GENESIS ensures that the interior nodes are relocated in a manner that minimises the distortion of individual elements as evident in the perturbed models shown in Figure 4(d). Once the perturbed mesh is found, the model is converted into the LS-DYNA format for crash simulations.

## 6.2 Description of random variables

In design of vehicle structures for crashworthiness, typical uncertainties include the collision scenario (e.g., impact velocity and offset distance) as well as the variability in material properties and geometric shape and size of structural components.

Many engineering materials used in automotive applications are polycrystalline in nature, and the presence of crystallographic characteristics, such as texture and misorientation, affects several important physical properties. Although these properties may have little or no influence at low deformation-rate applications, they often have destructive impact in high-rate applications such as crash.

Figure 5(a) shows the effect of strain rate on the true stress–strain curve. As suggested by Horstemeyer et al. (2005), small variability (~1%) in microstructures can result in very large (~13%) variation in failure stress. Here, we quantify material uncertainty due to microstructural features, manufacturing processes and their history effects by using an uncertainty stress–strain parameter defined by random variable  $X_1$ . This random variable is assumed to have a lognormal distribution and it describes the variability in the plastic portion of material stress–strain curves, as illustrated in Figure 5(b). The second random variable,  $X_2$ , defines the collision speed with a mean value of 15.65 m/s (35 mph) assuming a normal distribution with the direction of impact perpendicular to the barrier. Since in an OFI only a fraction of the vehicle front end comes in contact with the barrier, the offset distance is also treated as a normally distributed random variable, defined by  $X_3$ . In the case of  $X_3$ , a large Coefficient of Variation (COV) is meant to reflect a more realistic variation of offset distance in frontal collisions. The last random variable,  $X_4$ , captures the variability in occupant mass. Although it represents only a small fraction of the vehicle mass, it does have an influence on the kinetic energy of the vehicle.  $X_4$  is also assumed to have a normal probability distribution. The choice of distribution types represents an assumption on our part based on the available information. Table 2 gives the listing of the design and random variables with associated bounds and statistical properties, respectively.

**Figure 5** (a) Effect of strain rate on material constitutive relationship and (b) the band of uncertainty

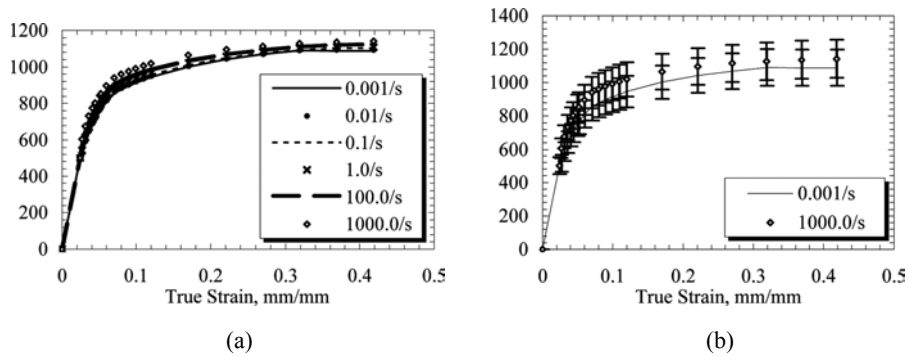


**Table 2** Description of design and random variables

Variable name (units)	Variable symbol	Lower bound	Upper bound	Mean	COV	Distribution type
Shape design variables	$Y_1 - Y_4$	-25.0	25.0	-	-	-
Wall Thickness (mm)	$Y_5$	0.75	1.25	-	-	-
Stress-strain parameter	$X_1$	-	-	1.0	0.033	Lognormal
Speed (m/s)	$X_2$	-	-	15.65	0.067	Normal
Offset distance (%)	$X_3$	-	-	40.0	0.167	Normal
Occupant mass (kg)	$X_4$	-	-	136.2	0.167	Normal

### 6.3 Metamodels for different responses

The 13 responses considered in this problem are the rail mass (Mass\_R), average intrusion distances at FP, DS, and steering wheel locations (Dis\_FP, Dis\_DS and Dis\_SW, respectively) in FFI and OFI, and average peak accelerations at the same three locations (Acc\_FP, Acc\_DS and Acc\_SW, respectively) in FFI and OFI. Since the FFI and OFI collision conditions are distinct from each other, a separate metamodel needs to be developed for each intrusion distance and acceleration response. The input variables for each model are those identified in Table 2, with  $X_3$  excluded in FFI-based metamodels.

Using the Latin Hypercube Sampling (LHS), a pool of 100 design (training) points is identified. Two crash simulations are performed at each training point, with the generated responses used in the development of PRS and RBF metamodels. An additional 40 randomly selected design points are used as test points to compare the exact and the estimated values of each response to validate the developed metamodels.

As a single global metric of accuracy, we used an average error estimate calculated as

$$\varepsilon = \frac{1}{N} \sum_{i=1}^N \frac{|f_i - \tilde{f}_i|}{f_i} \quad (9)$$

where  $N$  represents the total number of test design points (40 in this problem). Table 3 compares the average error estimates for the 13 responses. Generally, RBF models are superior to the PRS models with a few exceptions, the most noteworthy being the mass. The superiority of RBF is more evident in FFI than the OFI conditions. The greatest difference between the two models is in prediction of Dis\_SW, with the average error in RBF being approximately half that for PRS.

**Table 3** Comparison of average error in different metamodels

Response	FFI		OFI	
	$\varepsilon_{RBF}$ (%)	$\varepsilon_{PRS}$ (%)	$\varepsilon_{RBF}$ (%)	$\varepsilon_{PRS}$ (%)
Dis_FP	6.7	8.4	5.9	6.1
Dis_DS	6.7	8.3	8.4	7.8
Dis_SW	7.1	11.9	8.3	17.2
Acc_FP	5.7	9.1	5.2	5.0
Acc_DS	7.6	9.2	7.6	9.3
Acc_SW	5.0	6.4	3.8	3.6
Mass_R	1.1	0.2	1.1	0.2

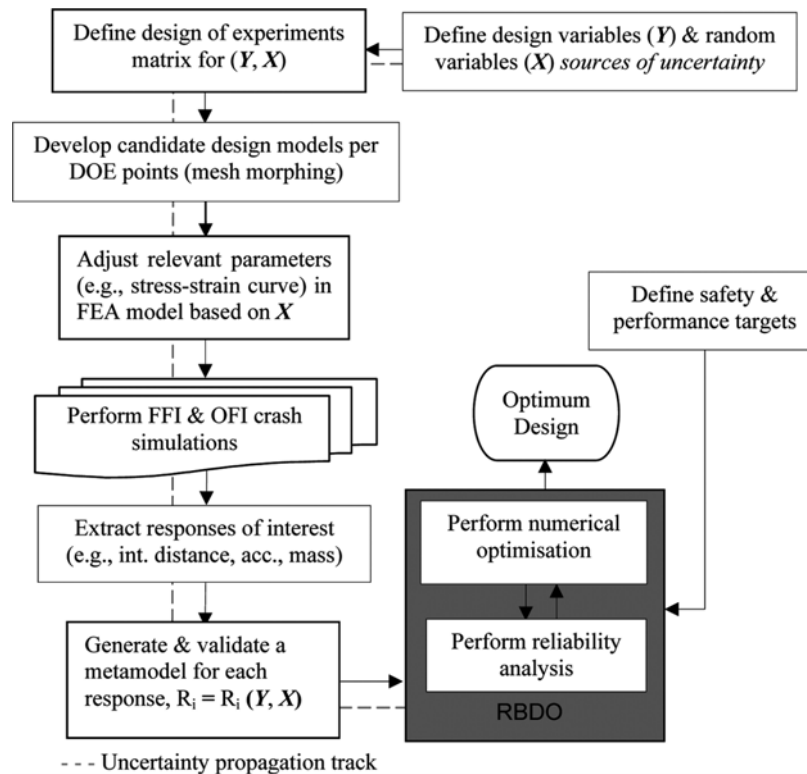
Although for all responses, RBF models consisted of 100 terms (see equation (6)), the number of terms in PRS models varied from one response to another as well as the crash condition. For example, for FFI, all PRS equations were second-order and had from 8–20 terms whereas in the case of OFI, they were second-order with 9–24 terms. On the basis of the functional characteristics of the responses of interest and the desire to use a single global metamodel for each response over the entire design space, we chose RBF for all intrusion distance and acceleration responses and PRS for structural mass.

We also investigated the effect of population size of training points as well as the area over which the intrusion distance and acceleration responses are averaged, and found that for most responses, 70 sample points provided acceptable accuracy with marginal improvement when nearing 100 samples. We also found that an increase of 50% in the surface area used for averaging of each crash response did not have any significant effect on the accuracy of the metamodels.

#### 6.4 Optimisation algorithm

The algorithm for crashworthiness optimisation based on RBDO formulation is described by the flowchart in Figure 6. It essentially involves five main elements: mesh morphing, crash simulations, metamodeling, structural reliability analysis and numerical optimisation. For the DDO solution, the algorithm is simplified with the elimination of reliability analysis and the random variables.

**Figure 6** Flowchart for the crashworthiness optimisation based on RBDO formulation



#### 6.5 DDO results and discussion

The metamodel-based DDO problem is solved using MMFD in VisualDOC (2005) while considering different choices for the design constraint set as well as the objective function. Table 4 gives a summary of the optimisation results for the rail mass minimisation (Mass\_R), single-site-single-crash scenario acceleration minimisation

(Acc\_FP\_F, Acc\_DS\_F, Acc\_SW\_F, Acc\_FP\_O, Acc\_DS\_O, Acc\_SW\_O) and the multi-objective acceleration minimisation (M\_Obj) problems.

**Table 4** Summary of DDO results

Variable/ response (units)	Baseline		Response minimised						
	model	Mass_R	Acc_FP_F	Acc_DS_F	Acc_SW_F	Acc_FP_O	Acc_DS_O	Acc_SW_O	M_Obj
$Y_1$	0.0	7.84	17.30	3.76	-1.62	4.23	3.26	12.36	9.02
$Y_2$	0.0	7.01	5.76	6.79	6.24	3.52	8.19	9.30	7.53
$Y_3$	0.0	2.27	3.06	2.50	-0.10	1.64	-1.17	-1.37	0.16
$Y_4$	0.0	-2.53	-4.81	-3.45	-2.30	-1.30	0.74	-0.58	-0.31
$Y_5$ (mm)	1.0	0.97	0.97	0.98	1.00	0.98	1.01	0.98	0.99
Mass_R (kg)	2.33	2.22	2.24	2.26	2.32	2.28	2.35	2.26	2.27
Acc_FP_F (mm/s <sup>2</sup> )	424844	382434	369332	389831	406573	391035	394834	377865	382291
Acc_DS_F (mm/s <sup>2</sup> )	687421	640011	667753	638321	653161	651072	661671	651425	650766
Acc_SW_F (mm/s <sup>2</sup> )	585434	566681	576182	567973	563881	573140	576396	566472	571718
Dis_FP_F (mm)	59.1	60.88	57.65	60.70	60.00	61.15	59.93	59.58	60.12
Dis_DS_F (mm)	40.5	41.58	39.06	41.39	40.49	41.82	41.12	40.57	41.13
Dis_SW_F (mm)	8.9	9.13	8.35	9.12	9.12	9.12	9.11	9.14	9.12
Acc_FP_O (mm/s <sup>2</sup> )	514641	502729	502549	502823	503177	501454	501752	502730	501814
Acc_DS_O (mm/s <sup>2</sup> )	933830	915513	918274	906207	916534	916247	884733	916625	904270
Acc_SW_O (mm/s <sup>2</sup> )	529007	507855	510428	510189	513155	513217	511981	504915	508790
Dis_FP_O (mm)	69.7	69.76	69.05	69.69	69.69	70.39	69.49	68.89	69.55
Dis_DS_O (mm)	55.2	50.62	50.89	50.55	50.78	51.48	50.96	50.40	50.93
Dis_SW_O (mm)	6.2	6.07	6.05	6.08	6.04	6.05	6.06	6.06	6.06

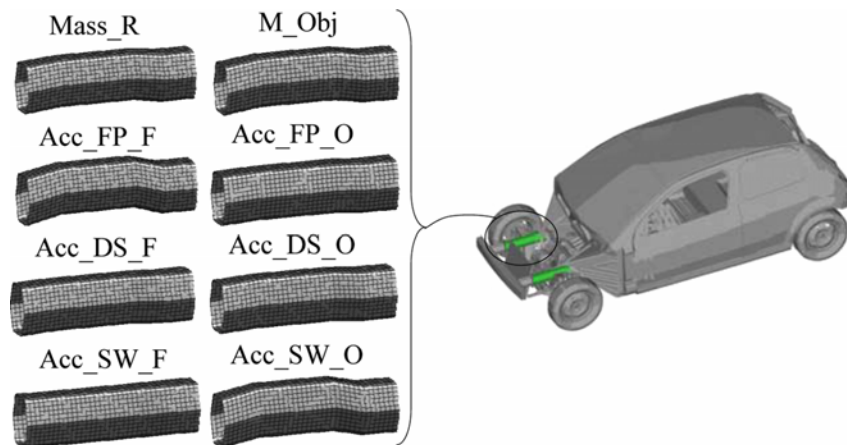
In each single-objective optimisation problem, there are 12 constraints with the bounds set equal to the corresponding responses in the baseline model. The solutions to these problems give an indication of how much a selected response can be improved over that of the baseline model. In the multi-objective optimisation (M\_Obj) problem, the six acceleration responses are combined using equation (2) to form a composite objective function while the remaining seven responses are treated as design constraints. The target acceleration values in equation (2) are those found through single-objective minimisation solutions whereas the worst values are set equal to the responses of the baseline model.

As was the case with the baseline model, in all DDO solutions, the largest intrusion distance occurs at the FP location whereas the maximum average acceleration occurs at the DS location.

The optimum side-rail geometry for each case is shown in Figure 7. Judging by the optimal shapes and values of  $Y_1$  through  $Y_4$ , it appears that the first and second GPV sets are considerably more influential than the other two. The thickness design variable remains relatively constant from one optimum design to another. Changing the optimisation method to SQP and using alternative initial design points did not produce any significant improvement in the optimisation results.

To measure the accuracy of the individual response values in Table 4, an FFI and OFI simulation was performed on each optimal design configuration, and the largest error was found to be less than 7% with the majority of responses having errors of less than 2%. It is important to note that the error in responses of optimum designs is less than the predicted error of individual metamodelling in Table 3.

**Figure 7** Optimal rail shapes based on DDO solutions (see online version for colours)

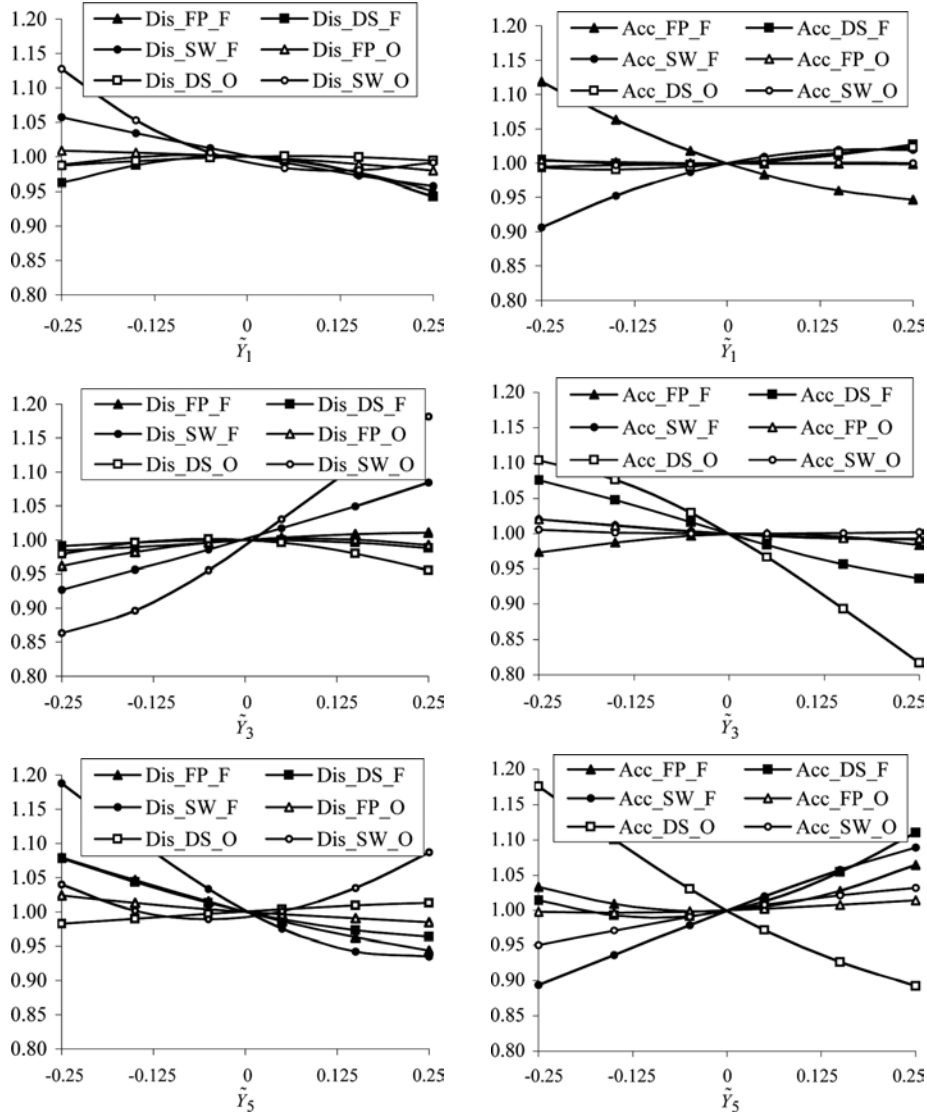


## 6.6 Design sensitivity analysis

The influence of design variables on intrusion distance and acceleration responses was examined through a design sensitivity analysis of the baseline model. The plots of normalised responses vs. normalised perturbations in  $Y_1$ ,  $Y_3$  and  $Y_5$  are shown in Figure 8. The responses are based on the corresponding RBF predictions and are normalised using the RBF-predicted values for the baseline model. The design variables are also normalised such that a value of zero represents the baseline model. The plots for  $Y_2$  and  $Y_4$  are similar to those of  $Y_1$  and  $Y_3$ , hence, not shown here.

The plots in Figure 8 reveal that, in many instances, increasing or decreasing a design variable from its baseline value will improve some responses (i.e., normalised response value less than 1.0) while worsening others (i.e., normalised response value greater than 1.0). This contradictory effect explains the limited amounts of mass and performance improvements that could be achieved by changing the rail geometry (especially wall thickness) during the optimisation process as observed in the DDO results. As noted previously, changing the initial design point or the method of solution did not have a significant impact on the optimisation results.

**Figure 8** Effect of changes in design variables 1, 3, and 5 on FFI and OFI responses



### 6.7 RBDO results and discussion

The RBDO problem based on equation (5) is solved using the SQP algorithm in MATLAB. Since the consequence of imposing limits on one or more responses (at a single vs. multiple sites) and the treatment of some constraints as deterministic and others as probabilistic is not necessarily intuitive, multiple optimisation problems are considered. A detailed comparison of results from different RBDO problems is also helpful to identify the influence of uncertainties in material properties and crash conditions on optimum design and to explore trade-offs between weight reduction and safety.

Table 5 gives the summary of RBDO results for most of the cases examined with configuration of each optimum design shown in Figure 9. In all the cases considered, the deterministic mass of the rail is minimised subject to a different combination of deterministic and probabilistic design constraints as identified in Table 5. While the deterministic constraints are bounded by the response values in the baseline model, the reliability-based constraints seek an improvement over the baseline model according to the selected target reliability index. The value of  $\beta_{t-max}$  indicates the largest target reliability index that we were able to impose on the probabilistic constraints and find an optimum solution. As a reference, when  $\beta=0$ , the response of the optimum design matches that of the baseline model whereas a positive or negative value indicates an improvement or worsening (i.e.,  $P_f > 0.5$ ) of the response with the magnitude of  $\beta$  indicating the extent of difference. Whenever a response is constrained, it is done so for both the FFI and the OFI conditions.

**Figure 9** Optimal rail shapes based on RBDO solutions (see online version for colours)

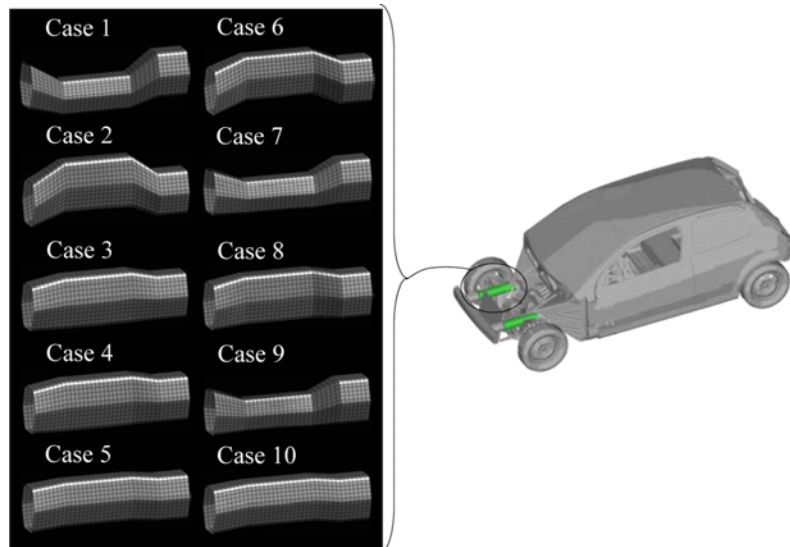


**Table 5** Summary of RBDO results

Variable/response	RBDO Solution				
	Case 1	Case 2	Case 3	Case 4	Case 5
	$\beta_{t-max} = 3.5$	$\beta_{t-max} = 2.5$	$\beta_{t-max} = 1.5$	$\beta_{t-max} = 1.5$	$\beta_{t-max} = 0.15$
$Y_1$	-22.53	23.73	-2.39	-2.90	5.24
$Y_2$	14.92	8.43	3.30	10.16	6.54
$Y_3$	25.0	-20.92	-15.75	-13.70	-1.81
$Y_4$	-4.28	19.54	-6.35	-9.30	0.13
$Y_5$ (mm)	0.93	1.04	0.97	1.00	1.00
Mass_R (kg)	1.95	2.49	2.38	2.41	2.33
$\beta_{Dis\_FP\_F}$	1.05	2.54 <sup>a</sup>	0.70	1.50 <sup>a</sup>	0.66 <sup>a</sup>

**Table 5** Summary of RBDO results (continued)

Variable/response	RBDO Solution				
	Case 1	Case 2	Case 3	Case 4	Case 5
	$\beta_{t-max} = 3.5$	$\beta_{t-max} = 2.5$	$\beta_{t-max} = 1.5$	$\beta_{t-max} = 1.5$	$\beta_{t-max} = 0.15$
$\beta_{Dis\_DS\_F}$	3.50 <sup>a</sup>	4.18	0.67	1.76 <sup>a</sup>	1.02 <sup>a</sup>
$\beta_{Dis\_DS\_F}$	3.50 <sup>a</sup>	4.18	0.67	1.76 <sup>a</sup>	1.02 <sup>a</sup>
$\beta_{Dis\_SW\_F}$	-5.54	-4.51	1.50 <sup>a</sup>	1.50 <sup>a</sup>	0.15 <sup>a</sup>
Acc_FP_F (mm/s <sup>2</sup> )	447540	409410 <sup>a</sup>	397150	406090	389410 <sup>a</sup>
Acc_DS_F (mm/s <sup>2</sup> )	667490 <sup>a</sup>	749400	703690	683710	661190 <sup>a</sup>
Acc_SW_F (mm/s <sup>2</sup> )	429990	518630	576280 <sup>a</sup>	573330	576050 <sup>a</sup>
$\beta_{Dis\_FP\_O}$	0.94	2.56 <sup>a</sup>	1.41	2.01 <sup>a</sup>	0.36 <sup>a</sup>
$\beta_{Dis\_DS\_O}$	3.50 <sup>a</sup>	2.20	0.97	1.50 <sup>a</sup>	0.30 <sup>a</sup>
$\beta_{Dis\_SW\_O}$	-6.20	-2.13	1.50 <sup>a</sup>	1.50 <sup>a</sup>	0.15 <sup>a</sup>
Acc_FP_O (mm/s <sup>2</sup> )	482710	503740 <sup>a</sup>	526570	528450	502590 <sup>a</sup>
Acc_DS_O (mm/s <sup>2</sup> )	890820 <sup>a</sup>	867420	1071600	1039600	916270 <sup>a</sup>
Acc_SW_O (mm/s <sup>2</sup> )	491840	499240	518030 <sup>a</sup>	515940	511660 <sup>a</sup>
	Case 6	Case 7	Case 8	Case 9	Case 10
	$\beta_{t-max} = 1.0$	$\beta_{t-max} = 1.0$	$\beta_{t-max} = 1.75$	$\beta_{t-max} = 0.75$	$\beta_{t-max} = 0.07$
$Y_1$	25.00	-5.56	2.55	-3.03	7.77
$Y_2$	25.00	8.83	20.92	16.59	4.19
$Y_3$	2.41	25.00	-7.81	24.48	0.48
$Y_4$	-13.35	12.92	-6.70	23.34	0.44
$Y_5$ (mm)	0.86	0.83	1.01	0.75	0.99
Mass_R (kg)	1.91	1.68	2.32	1.50	2.29
Dis_FP_F (mm)	63.1	60.5 <sup>a</sup>	58.8	58.5	60.5 <sup>a</sup>
Dis_DS_F (mm)	42.3 <sup>a</sup>	38.6	39.7	37.4	41.4 <sup>a</sup>
Dis_SW_F (mm)	10.5	13.7	9.1 <sup>a</sup>	14.6	9.1 <sup>a</sup>
$\beta_{Acc\_FP\_F}$	0.22	0.99 <sup>a</sup>	-0.47	0.75 <sup>a</sup>	0.90 <sup>a</sup>
$\beta_{Acc\_DS\_F}$	1.00 <sup>a</sup>	-0.23	0.33	1.08 <sup>a</sup>	0.18 <sup>a</sup>
$\beta_{Acc\_SW\_F}$	3.92	3.49	1.78 <sup>a</sup>	4.60 <sup>a</sup>	0.07 <sup>a</sup>
Dis_FP_O (mm)	67.4	67.7 <sup>a</sup>	63.7	68.5	70.2 <sup>a</sup>
Dis_DS_O (mm)	45.2 <sup>a</sup>	43.0	44.5	44.1	51.6 <sup>a</sup>
Dis_SW_O (mm)	7.8	9.3	6.1 <sup>a</sup>	10.6	6.1 <sup>a</sup>
$\beta_{Acc\_FP\_O}$	-0.54	0.99 <sup>a</sup>	-0.60	0.75 <sup>a</sup>	0.07 <sup>a</sup>
$\beta_{Acc\_DS\_O}$	1.00 <sup>a</sup>	2.47	-0.92	1.71 <sup>a</sup>	0.07 <sup>a</sup>
$\beta_{Acc\_SW\_O}$	2.05	2.34	1.74 <sup>a</sup>	3.27 <sup>a</sup>	0.51 <sup>a</sup>

<sup>a</sup>Response treated as a design constraint.

Some general observations based on the RBDO results are summarised as follows:

- The  $\beta_{r\text{-max}}$  values for the cases with single-site constraints are generally higher than those having multi-site constraints. This is true regardless of whether intrusion distance or acceleration responses are treated as probabilistic.
- When only the intrusion distance responses are treated as probabilistic (cases 1 through 5), the  $\beta_{r\text{-max}}$  values are mostly higher than those in the corresponding cases with acceleration responses treated as probabilistic (cases 6–10). This trend implies that reliability-based acceleration constraints impose more stringent limits on the rail design than do the intrusion distance constraints of the same type.
- Amongst the three sites considered, imposing a probabilistic constraint on the intrusion distance at the steering wheel location is more demanding than the same constraint at any of the other two sites. By constraining Dis\_SW, the intrusion distances at the other locations also improve whereas the opposite is not true. A similar pattern does not appear to exist for the acceleration responses indicating that a single-site acceleration constraint is not appropriate.
- Comparison of cases 5 and 10 indicates that it is possible to improve design safety with little or no mass penalty. However, both the mass savings and the safety improvements are modest in comparison with the baseline model owing to the conflicting influence of design variables and sensitivity patterns as shown in Figure 8.
- In all the cases, the optimiser changed the shape of the rail into a non-prismatic geometry with varying degrees of contribution from each GPV set.
- When treating all 12 intrusion distance and acceleration constraints as probabilistic (not shown in Table 5), we found  $\beta_{r\text{-max}} = 0.04$  for a minimum side-rail mass of 2.277 lb.

### 6.8 Effect of error in metamodel on reliability estimates and RBDO results

As noted earlier, we found the largest error in the metamodel predicted responses of the deterministic optimum models to be around 7% with the majority of responses having errors of less than 2%. These errors are actually smaller than the average errors for the individual metamodels in Table 3.

For reliability estimation, a response prediction error may lead to a larger or smaller error in  $\beta$  depending on the extent of the non-linearity of the response function, as well as the error in the response function at the point where the MPP is evaluated. However, given the level of non-linearity in the car crash responses and the unlikelihood that the critical region used for reliability calculation (i.e., at the MPP) aligns with the region of maximum error found in the response functions, it is expected that error in metamodel based  $\beta$  is in the same range as those found in deterministic responses. It is – of course – possible to calculate this error exactly, but the computational demand for this type of problem is quite high.

It is also worth noting that if we were to directly link FE simulations with AMV+ reliability analysis and design optimisation (overlooking the numerical difficulties), we would still encounter another source of error owing to the finite-difference estimation

of response derivatives that appear in both the reliability analysis and the design optimisation. However, this error can be eliminated when using analytical metamodels. Otherwise, the procedures used in RBDO remain the same whether we use the exact or metamodel-based responses.

## 7 Summary and conclusions

In this paper, the effects of deterministic and probabilistic (reliability-based) design constraints on shape and sizing optimisation of an automotive component were investigated. While the inclusion of design uncertainties in probabilistic formulation and RBDO can boost confidence in the structural safety predictions, the mathematical complexity of the corresponding optimisation problem tends to increase the computational cost. This is particularly true when the response functions are highly non-linear and require the use of high-fidelity FE simulations of a complex physical phenomenon such as crash. The development of analytical surrogate models to increase the efficiency of crashworthiness optimisation was a crucial element in the overall structural optimisation scheme.

The metamodel-based design methodology was applied to structural optimisation of the rail component of a passenger car under full- and offset-frontal crash scenarios. The metamodel-based optimum results were validated using FE simulations of full-vehicle crash scenarios. On the basis of the results of the crashworthiness optimisation problem, it appears that the choice of single vs. multi-site constraints and the modelling of constraints as deterministic or probabilistic have the greatest impact on the component design. While adjusting the shape of the rail was effective, the effects of rail geometry on the vehicle responses considered were mixed resulting in moderate design improvements. Future efforts will explore the expansion of the design space to include other components besides the rail in structural optimisation and energy absorption management. Also, other important design considerations such as manufacturability and process optimisation will be addressed.

## Acknowledgements

This material is based on the work supported by the US Department of Energy under Award Number DE-FC26-06NT42755. The authors are also grateful to the reviewers for their helpful comments.

## References

- Acar, E. and Rais-Rohani, M. (2009) 'Ensemble of metamodels with optimized weight factors', *Structural and Multidisciplinary Optimization*, Vol. 37, No. 3, pp.279–294.
- Acar, E., Rais-Rohani, M. and Eamon, C. (2010) 'Structural reliability analysis using dimension reduction and extended generalized lambda distribution', *International Journal of Reliability and Safety*, Vol. 4, Nos. 2–3, pp.166–187.
- Agarwal, H., Mozumder, C.K., Renaud, J.E. and Watson, L.T. (2007) 'An inverse-measure-based unilevel architecture for reliability-based design optimization', *Structural and Multidisciplinary Optimization*, Vol. 33, No. 3, pp.217–227.

- Automotive Lightweighting Materials (2007) 2006 Annual Report, [http://www1.eere.energy.gov/vehiclesandfuels/resources/vt\\_alm\\_fy06.html](http://www1.eere.energy.gov/vehiclesandfuels/resources/vt_alm_fy06.html), October.
- Buhmann, M.D. (2003) *Radial Basis Functions: Theory and Implementations*, Cambridge University Press, New York, NY.
- Chen, X., Hasselman, T.K. and Neill, D.J. (1997) 'Reliability-based structural design optimization for practical applications', *Proceedings of the 38th AIAA/ASME/ASCE/AHS Structures, Structural Dynamics and Materials Conference*, 7–10 April, Kissimmee, FL.
- Choi, K.K., Tu, J. and Park, Y.H. (2001) 'Extensions of design potential concept for reliability-based design optimization to nonsmooth and extreme cases', *Structural and Multidisciplinary Optimization*, Vol. 22, pp.335–350.
- Daberkow, D.D. and Mavris, D.N. (2002) 'An investigation of metamodeling techniques for complex system design', *Proceedings of the 9th AIAA/ISSMO Symposium on Multidisciplinary Analysis and Optimization*, 4–6 September, Atlanta, GA.
- Darlington, R.B. (1990) *Regression and Linear Models*, McGraw-Hill, New York.
- Der Kiureghian, A., Lin, H.Z. and Hwang, S.J. (1987) 'Second-order reliability approximations', *Journal of Engineering Mechanics*, Vol. 113, No. 8, pp.1208–1225.
- Du, X. and Chen, W. (2004) 'Sequential optimization and reliability assessment method for efficient probabilistic design', *Journal of Mechanical Design*, Vol. 126, No. 2, pp.225–233.
- Enevoldsen, I. and Sorensen, J.D. (1994) 'Reliability-based optimization in structural engineering', *Structural Safety*, Vol. 15, pp.169–196.
- Fang, H., Rais-Rohani, M., Liu, Z. and Horstemeyer, M.F. (2005) 'A comparative study of metamodeling methods for multiobjective crashworthiness optimization', *Computers and Structures*, Vol. 83, pp.2121–2136.
- Fang, H., Solanki, K. and Horstemeyer, M.F. (2004) 'Numerical simulations of multiple vehicle crashes and multidisciplinary crashworthiness optimization', *International Journal of Crashworthiness*, Vol. 10, No. 2, pp.161–171.
- Federal Motor Vehicle Safety Standards and Regulations (1998) US Department of Transportation, National Highway Traffic Safety Administration, Washington DC.
- Frangopol, D.M. (1995) 'Reliability-based optimum structural design', in Sundararajan, C. (Ed.): *Probabilistic Structural Mechanics Handbook, Theory and Industrial Applications*, Chapman & Hall, New York, NY.
- GENESIS (2005) GENESIS User's Manual, Version 7.5, Vanderplaats Research & Development, Inc., Colorado Springs, CO.
- Goel, T., Haftka, R.T., Shyy, W. and Queipo, N.V. (2007) 'Ensemble of surrogates', *Journal of Structural and Multidisciplinary Optimization*, Vol. 33, No. 3, pp.199–216.
- Grandhi, R.V. and Wang, L. (1988) 'Reliability-based structural optimization using improved two-point adaptive non-linear approximation', *Finite Elements in Analysis and Design*, Vol. 29, pp.35–48.
- Gu, L. and Yang, R.J. (2006) 'On reliability-based optimisation methods for automotive structures', *International Journal of Materials and Product Technology*, Vol. 25, Nos. 1–3, pp.3–26.
- Hasofer, A.M. and Lind, N. (1974) 'An exact and invariant first-order reliability format', *Journal of Engineering Mechanics*, Vol. 100, No. EM1, pp.111–121.
- Horstemeyer, M.F., Solanki, K. and Steele, W.G. (2005) 'Uncertainty methodologies to characterize a damage evolution model', *Plasticity 2005 Conference*, 4–8 January, Kauai, Hawaii.
- Jin, R., Chen, W. and Simpson, T.W. (2001) 'Comparative studies of metamodeling techniques under multiple modeling criteria', *Structural and Multidisciplinary Optimization*, Vol. 23, No. 1, pp.1–13.

- Karian, Z.E., Dudewicz, E.J. and McDonald, P. (1996) 'The extended generalized lambda distribution system for fitting distributions to data: history, completion of theory, tables, applications, the 'final word' on moment fits', *Communications in Statistics – Computation and Simulation*, Vol. 25, No. 3, pp.611–642.
- Kaymaz, I. and McMahon, C.A. (2004) 'A probabilistic design system for reliability-based design optimization', *Structural and Multidisciplinary Optimization*, Vol. 28, pp.416–426.
- Kharmanda, G. and Olhoff, N. (2007) 'Extension of optimum safety factor method to non-linear reliability-based design optimisation', *Structural and Multidisciplinary Optimization*, Vol. 34, No. 5, pp.367–380.
- Kharmanda, G., Mohamed, A. and Lemaire, M. (2002) 'Efficient reliability-based design optimization using a hybrid space with application to finite element analysis', *Structural and Multidisciplinary Optimization*, Vol. 24, No. 3, pp.233–245.
- Kharmanda, G., Olhoff, N. and El-Hami, A. (2004) 'Optimum values of structural safety factors for a predefined reliability level with extension to multiple limit states', *Structural and Multidisciplinary Optimization*, Vol. 27, No. 6, pp.421–434.
- Kirjner-Neto, C., Polak, E. and Der Kiureghian, A. (1998) 'An outer approximations approach to reliability-based optimal design of structures', *Journal of Optimization Theory and Applications*, Vol. 98, No. 1, pp.1–16.
- Koch, P.N. and Kodiyalam, S. (1999) 'Variable complexity structural reliability analysis for efficient reliability-based design optimization', *Proceedings of the 40th AIAA/ASME/ASCE/AHS/ASC Structures, Structural Dynamics and Materials Conference*, 12–15 April, St. Louis, MO.
- Kuschel, N. and Rackwitz, R. (2000) 'A new approach for structural optimization of series systems', *Applications of Statistics and Probability*, Vol. 2, No. 8, pp.987–994.
- Lee, H. and Kwak, M. (1995) 'Reliability-based structural optimal design using the Neumann expansion technique', *Computers and Structures*, Vol. 55, No. 2, pp.287–296.
- Liaw, L.D. and DeVires, R.I. (2001) 'Reliability-based optimization for robust design', *International Journal of Vehicle Design*, Vol. 25, Nos. 1–2, pp.64–77.
- Liu, P-L. and Der Kiureghian, A. (1991) 'Optimization algorithms for structural safety', *Structural Safety*, Vol. 9, pp.161–177.
- Melchers, R.E. (1989) 'Importance sampling in structural systems', *Structural Safety*, Vol. 6, pp.3–10.
- Mohsine, A., Kharmanda, G. and El-Hami, A. (2004) 'Improved hybrid method as a robust tool for reliability-based design optimization', *Structural and Multidisciplinary Optimization*, Vol. 32, No. 3, pp.203–213.
- Nie, J. and Ellingwood, B.R. (2000) 'Directional methods for structural reliability analysis', *Structural Safety*, Vol. 22, pp.233–249.
- Papadrakakis, M. and Lagaros, N.D. (2002) 'Reliability-based structural optimization using neural networks and Monte Carlo simulation', *Computer Methods in Applied Mechanics and Engineering*, Vol. 191, pp.3491–3507.
- Qu, X. and Haftka, R.T. (2004) 'Reliability-based design optimization using probabilistic safety factor', *Structural and Multidisciplinary Optimization*, Vol. 27, No. 5, pp.314–325.
- Rackwitz, R. (2001) 'Reliability analysis – a review and some perspectives', *Structural Safety*, Vol. 23, pp.365–395.
- Rackwitz, R. and Fiessler, B. (1978) 'Structural reliability under combined load sequences', *Computers and Structures*, Vol. 9, pp.489–494.
- Rahman, S. and Xu, H. (2004) 'A univariate dimension-reduction method for multi-dimensional integration in stochastic mechanics', *Probabilistic Engineering Mechanics*, Vol. 19, pp.393–408.

- Rais-Rohani, M. and Singh, M.N. (2004) 'Comparison of global and local response surface techniques in reliability-based optimization of composite structures', *Structural and Multidisciplinary Optimization*, Vol. 26, No. 5, pp.333–345.
- Rais-Rohani, M., Solanki, K. and Eamon, C. (2006) 'Reliability-based optimization of lightweight automotive structures for crashworthiness', *Proceedings of the 11th AIAA/ISSMO Multidisciplinary Analysis and Optimization Conference*, 6–8 September, Portsmouth, VA.
- Rao, S.S. (1992) *Reliability-Based Design*, McGraw-Hill, Inc., New York, NY.
- Rao, S.S. (1996) *Engineering Optimization Theory and Practice*, 3rd ed., John Wiley & Sons, Inc., New York, NY.
- Rubinstein, R.Y. (1981) *Simulation and the Monte Carlo Method*, Wiley, New York, NY.
- Simpson, T.W., Mauery, T.M., Korte, J.J. and Mistree, F. (1998) 'Comparison of response surface and kriging models for multidisciplinary design optimization', *Proceedings of the 7th AIAA/USAF/NASA/ISSMO Symposium on Multidisciplinary Analysis and Optimization*, 2–4 September, St. Louis, MO.
- Simpson, T.W., Peplinski, J., Koch, P.N. and Allen, J.K. (2001) 'Metamodels for computer-based engineering design: survey and recommendations', *Engineering and Computers*, Vol. 17, No. 2, pp.129–150.
- Sinha, K. (2007) 'Reliability-based multiobjective optimization for automotive crashworthiness and occupant safety', *Structural and Multidisciplinary Optimization*, Vol. 33, No. 3, pp.255–268.
- Tu, J., Choi, K.K. and Park, Y.H. (1999) 'A new study on reliability based design optimization', *Journal of Mechanical Design*, Vol. 121, No. 4, pp.557–564.
- Vanderplaats, G.N. (1999) *Numerical Optimization Techniques for Engineering Design*, 3rd ed., Vanderplaats Research & Development, Inc., Colorado Springs, CO.
- VisualDOC (2005) VisualDOC User's Manual, version 5.1, Vanderplaats Research & Development, Inc., Colorado Springs, CO.
- Wang, L. and Grandhi, R.V. (1994) 'Efficient safety index calculation for structural reliability analysis', *Computers and Structures*, Vol. 54, pp.103–111.
- Wang, L., Beeson, D., Wiggs, G. and Rayasam, M. (2006) 'A comparison of meta-modeling methods using practical industry requirements', *Proceedings of the 47th AIAA/ASME/ASCE/AHS/ASC Structures, Structural Dynamics, and Materials Conference*, 1–4 May, Newport, RI.
- Wu, Y-T. (1994) 'Computational methods for efficient structural reliability and reliability sensitivity analysis', *AIAA Journal*, Vol. 32, No. 8, pp.1717–1723.
- Wu, Y-T. and Burnside, O.H. (1988) 'Efficient probabilistic structural analysis using an advanced mean value method', *Proceedings of ASCE Specialty Conference on Probabilistic Mechanics and Structural and Geotechnical Safety*, 25–27 May, Blacksburg, VA.
- Wu, Y-T. and Wirsching, P.H. (1987) 'New algorithm for structural reliability estimation', *Journal of Engineering Mechanics*, Vol. 113, No. 9, pp.1319–1336.
- Wu, Y-T., Millwater, H.R. and Cruse, T.A. (1990) 'An advanced probabilistic structural analysis method for implicit performance functions', *AIAA Journal*, Vol. 28, No. 9, pp.1840–1845.
- Yang, R.J. and Gu, L. (2004) 'Experience with approximate reliability-based optimization methods', *Structural and Multidisciplinary Optimization*, Vol. 26, Nos. 1–2, pp.152–159.
- Yang, R.J., Chuang, C., Gu, L. and Li, G. (2005) 'Experience with approximate reliability-based optimization methods ii: an exhaust system problem', *Structural and Multidisciplinary Optimization*, Vol. 29, pp.488–497.
- Yang, R.J., Gu, L., Soto, C., Li, G. and Tyan, T. (2004) 'Developments and applications of structural optimization and robustness methods in vehicle impacts', *Proceedings of ASME International Mechanical Engineering Congress and Exposition*, 13–20 November, Anaheim, CA.
- Youn, B.D. and Choi, K.K. (2004a) 'Selecting probabilistic approaches for reliability-based design optimization', *AIAA Journal*, Vol. 42, No. 1, pp.124–131.

- Youn, B.D. and Choi, K.K. (2004b) 'A new response surface methodology for reliability-based design optimization', *Computers and Structures*, Vol. 82, pp.241–256.
- Youn, B.D., Choi, K.K., Yang, R-J. and Gu, L. (2004) 'Reliability-based design optimization for crashworthiness of vehicle side impact', *Structural and Multidisciplinary Optimization*, Vol. 26, pp.272–283.
- Yu, X., Choi, K.K. and Chang, K. (1997) 'A mixed design approach for probabilistic structural durability', *Journal of Structural Optimization*, Vol. 14, Nos. 2–3, pp.81–90.
- Zhang, Y. and Liu, Q. (2002) 'Reliability-based design of automobile components', *Proceedings of the Institution of Mechanical Engineers, Part D: Journal of Automobile Engineering*, Vol. 216, No. 6, pp.455–471.
- Zou, T. and Mahadevan, S. (2006) 'A direct coupling approach for efficient reliability-based design optimization', *Structural and Multidisciplinary Optimization*, Vol. 31, No. 3, pp.190–200.